JOURNAL OF SPACECRAFT AND ROCKETS
Vol. 42, No. 4, July–August 2005

Electroactive-Polymer Actuators for Controlling Space Inflatable Structures

Steve Tung* and Scott Witherspoon†
University of Arkansas, Fayetteville, Arkansas 72701

Space inflatable structures present a unique challenge to the design of actuators that can be used to effectively control the surface contour of the structures for the purposes of health monitoring and damage detection. Any actuator designed for space inflatable must be highly flexible and have low mass so that the structural integrity of the inflatable will not be severely compromised by the attachment of the actuator. Among current actuator designs, electroactive-polymer-based actuators are the most promising ones. Electroactive polymer is a new class of "smart" material that can convert electrical energy into mechanical energy. Ionic polymer metal composites and conductive polymers, which belong to the electroactive polymer group, can be effective actuation materials because of their low activation voltage of about 5 V and potentially large strains. Both types of actuators were fabricated, and their stress and strain outputs evaluated for use on inflatable structures.

Nomenclature

C_V	=	volume capacitance
D	=	ionic diffusion coefficient
d, y, F, M	=	actuator's deflection, tip deflection, point force, and moment, respectively
i_d	=	current density
L, L_{eff}, l	=	actuator's neutral length, effective length, and instantaneous length, respectively
q	=	charge consumed
R_e	=	electrolyte resistance
t_a, I_a, E_a	=	actuator's thickness, moment of inertia, and elastic modulus, respectively
t_s, I_s, E_s	=	shell's thickness, moment of inertia, and elastic modulus, respectively
ε, ε_f	=	actuator's axial-strain and free-strain capability
η	=	conductivity
κ	=	curvature
ρ	=	radius
σ	=	stress output
τ_D	=	diffusion time constant
τ_{RC}	=	resistance-capacitance time constant

Introduction

IT was recently noted that the increasing degree of complexity and sophistication in space exploration has demanded space systems to "meet expanded flight performance requirements, recover from failure or a serious mission degradation event, increase reliability, and reduce overall system cost."[1] For inflatable structures, this means incorporating health monitoring and control capabilities into the structure. A control system for inflatable structures requires actuators that are highly flexible and have low mass.

Electroactive polymer (EAP) is a class of flexible actuators that can convert electrical energy into mechanical energy. EAP materials such as polyvinylidene fluoride (PVDF) have been previously demonstrated to be effective in shape control of inflatable structures.[2] However, PVDF requires a large activation voltage (∼1000 V) and can only supply a small strain.

One class of low voltage (∼5 V) EAP is the ionic polymer metal composite (IPMC). An IPMC consists of a polymeric ion exchange membrane with metallic electrodes on each side. An electric field applied through the metal electrodes causes ions to migrate across the membrane. When this occurs, water molecules in the membrane migrate with the ions as a result of electrophoretic "dragging," causing the polymer to swell on one side and shrink on the other. This results in an overall bending motion in the IPMC. IPMC actuators exhibit large strains on the order of 1–10% at voltages less than 10 V (Ref. 3).

Another class of low-voltage EAP is conductive polymer (CP). CPs, such as polypyrrole (PPy), are intrinsically conductive. When surrounded by an electrolyte, CP can expand or contract when ions migrate in and out of the polymer. Ion migration occurs when it is oxidized or reduced by an applied current. Similar to IPMC, CP can also provide large strains at low voltages.[3] To form a bending actuator, a nonactive polymer membrane can be laminated to one side of the CP actuator, forcing the actuator to expand unevenly across the active CP layer. Two types of EAP actuators, one IPMC and the other CP based, were fabricated and evaluated against the stress and strain requirements for controlling a rigidized truss member.

Design Criteria

To determine whether IMPC or CP actuators can be effective in controlling space inflatable structures, it is necessary to first determine the design criteria for the EAP actuators in terms of stress and strain output requirements. This can be accomplished by modeling the interaction between a typical truss member of a space inflatable structure and the actuator "patch" attached to it. Detailed modeling of inflatable structures is complex because of geometry and nonlinearity. Large structure displacements cause nonlinear behavior with respect to the force-displacement curve. Also, the polyimide material of the inflatable structure exhibits a nonlinear relation of modulus with respect to frequency and inflation pressure.[4]

However, localized actuator/shell interaction can be estimated if the local area of a shell is assumed to be a small straight beam as shown in Fig. 1.

If the actuator patch is assumed to be perfectly laminated, the interaction between the structure and actuator patch can be estimated by a simplified pin-force model. A full derivation and discussion can be found in Chaudhry and Rogers.[5] In this model, the actuator is considered to provide a point force at the edge of the actuator. This force creates a moment M that can be related to the curvature of the

Presented as Paper 2003-1714 at the AIAA/ASME/ASCE/AHS/ASC 44th Structures, Structural Dynamics, and Materials Conference, Norfolk, VA, 7–10 April 2003; received 18 June 2003; revision received 8 May 2004; accepted for publication 10 June 2004.

*Assistant Professor, Department of Mechanical Engineering. Member AIAA.

†Graduate Research Assistant, Department of Mechanical Engineering. Student Member AIAA.

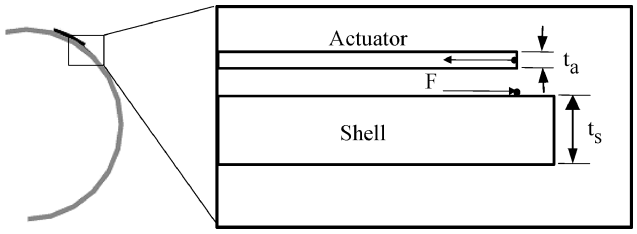

Fig. 1 Pin-force model for actuator/shell structure.

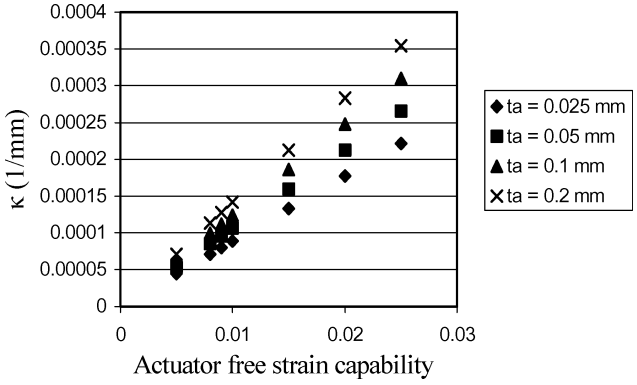

Fig. 2 Shell curvature vs actuator free-strain capability for varying actuator thickness.

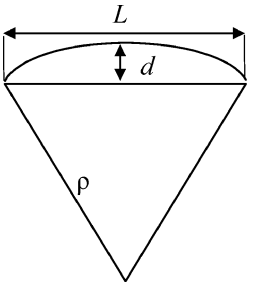

Fig. 3 Geometry of the actuator-induced curvature.

idealized beam by

$$M = F(t_s/2) = (E_s I_s)\kappa \tag{1}$$

where $E_s I_s$ is the shell rigidity. By equating the induced strains of the actuator and shell at the edge of the actuator, the curvature of the beam can be estimated by the free-strain capabilities of the actuator ε_f by the equation

$$\kappa = 6\varepsilon_f / t_s(3 + \psi) \tag{2}$$

where $\psi = (E_s t_s)/(E_a t_a)$. The pin-force model is valid for thickness ratios (t_s/t_a) greater than six.

Figure 2 shows the relationship between the actuator-induced strain in the shell and the actuator's free-strain capability for different actuator thickness. Shell properties used in the calculations, $E_s = 6.9$ GPa, $t_s = 350$ μm, and $E_a = 50$ MPa, are those of typical rigidized materials.[6] The actuator modulus is that of PPy (50 MPa) (Ref. 7). As demonstrated by the figure, the actuator-induced curvature scales linearly with the actuator's free-strain capability for all actuator thickness. Based on this figure, the actuator strain output requirement can be determined by assuming that it is necessary to deflect the surface of the truss by 0.1% of the diameter of the truss member (22 mm) in order to achieve effective control.

Figure 3 shows the geometry of the actuator-induced curvature κ (radius $= \rho$) when the actuator of length L deflects by d. Based on this figure, the relationship between κ and d can be described by

$$\kappa = \left[\tfrac{1}{2}(L^2/4d + d)\right]^{-1} \tag{3}$$

Assuming that it is necessary to deflect the surface of the truss by 0.1% of the diameter of the truss member (22 mm) to achieve effective control, the change of curvature requirement becomes 10^{-4} mm^{-1} for a 20-mm-long actuator patch. To achieve this curvature, based on Fig. 2, the actuator free-strain requirement is approximately 0.008 to 0.01 for an actuator thickness between 0.025 and 0.2 mm.

Equation (1) can be used to determine the actuator stress requirement from the curvature calculated using Eq. (3). Based on a curvature of 10^{-4} mm^{-1}, the force requirement is approximately 14 mN/mm of thickness, which corresponds to a stress requirement of 0.5 MPa for a 25-μm-thick actuator.

Fabrication Methods

The IPMC actuator was fabricated by metalizing a 185-μm-thick Nafion™-117 membrane with a triple-layered structure of Ti, Cu, and Au. The Ti and Cu layers were thin seed layers (0.05 and 0.25 μm thick, respectively) deposited by sputtering. The Au layer was 2 μm thick and was deposited by electroplating. After both sides were metallized, the membrane was cut into small strips for testing. The combined actuator thickness was approximately 190 μm. The IPMC metallic layers showed good adhesion under all normal testing conditions.

The CP actuator was realized through the oxidation of a pyrrole monomer and the incorporation of an anion into the polymeric chain to form PPy. Polymerization followed the reaction

$$C_4H_5N + A^- \rightarrow C_4H_5N^+A^- \tag{4}$$

The process was carried out in an electrochemical cell using a solution of 0.1 M pyrrole and 0.1 M tetrabutylammonium tetrafluoroborate (TBA-BF_4) dissolved in analytical grade acetonitrile. Polished Pt electrodes (20×8 mm) were used as the cathode and anode. A constant current level of 1–2.5 mA/cm^2 was employed in the cell. In electrochemical polymerization, the applied current caused the monomers to oxidize and crosslink, forming an insoluble polymeric chain on the anode.

The amount of charge passed was used to control the film thickness. The membrane thickness followed a linear relation with the charge passed. Fabrication of the PPy membranes was carried out by passing a charge of 13–16 C. At this charge level, consistent membranes 20–25 μm thick were fabricated. After combining with a nonactive membrane, the total CP actuators were approximately 90 μm thick.

Experimental Setup

Electromechanical testing of the IPMC actuator was carried out with the actuator positioned as a cantilevered beam in a plastic clamp with embedded Pt contacts. The Pt contacts provided electrical contact with the IPMC. For testing, the actuator was first soaked in deionized water for 24 h, removed, and immediately tested in air.

The applied potential required for ion migration and full actuation was quite small, typically less than 4 V. In fact, the applied potential was limited by the onset of electrolysis: the separation of water molecules into their ionic species of H^+ and OH^-. In this unwanted chemical reaction, actuator performance suffered, and hydrogen gas evolved from the IPMC membrane causing damage to the surface electrodes. The standard potential for hydrolysis to occur is 1.23 V, but evolution of gas in the IPMC typically did not occur until ±4 V was reached. When the IPMC actuator was activated above the ±4 V hydrolysis limit, delamination of the metallic layers occurred because of hydrogen gas formation from hydrolysis.

The electromechanical performance of the CP actuator was examined in an aqueous electrolyte of 0.1 M $LiClO_4$. The actuator was positioned in a cantilevered configuration similar to the IPMC. A platinum electrode placed at a distance of 10 mm was used as the counter electrode, and a cathodic or anodic current was applied to the active polymer. The current was ramped up to 1–2 mA/cm^2.

The bending was possible to achieve because the CP actuator was constructed of one active layer and one nonactive polymer layer that restricted the PPy expansion and contraction causing bending. The applied current determines the amount of oxidation and reduction. The y deflection, or the transverse displacement, was measured by

a laser displacement sensor (Keyence LK-031). The sensor could measure small displacements accurately up to ±0.01 mm, but the measurement range was limited to ±2 mm in the y direction as a result of the actuator bending out of the line of sight of the laser.

A force testing station was designed specifically for measuring the tip force of the actuator. The load cell had a maximum range of 30 g and a maximum resolution is approximately 0.2 mN, which is about 5% of the expected maximum tip force. Because of this, a lever was used to mechanically transfer the force output from the actuator tip to the load cell. To improve this number, the lever was designed to provide a gain of approximately 18.5. At this gain level, the resolution became 0.01 mN, or 0.25% of the expected tip force. The testing station was then able to measure a maximum force of approximately 15 mN.

Results and Discussion

IPMC Actuator

When a voltage bias was applied to the cantilever IPMC actuator, the actuator strip deflected toward the side of the negatively biased electrode as shown in Fig. 4. The displacement angle θ was measured by drawing a line from the free end of the actuator to its base as shown in Fig. 5. An actuator measuring 2 × 45 mm was tested. The angles of deflection from a strip that measured at different dc biasing voltages are shown in Fig. 6. A maximum deflection angle of 45 deg was achieved at −4 V. It can be seen that the actuator deflection is the largest towards the base where the voltage bias is applied. This is expected because of a voltage drop from the base to the free end of the actuator as a result of the nonzero electrical resistance of the metal layers in the IPMC.

The IPMC actuator deflected fairly linearly with respect to the bias voltage in the positive voltage regime as expected,[8] but in the opposite direction the deflection was nonlinear with respect to voltage. Also, the maximum deflection angle in one direction did not match the maximum deflection angle in the other direction. The unexpected results were probably caused by fabrication errors and uncertainties. One possible explanation might have been uneven thickness in the metal electrode layers. Another possibility was one electrode in the actuator being damaged by the rf etch or metal sputtering during the deposition of the other electrode.

When tested in air, evaporation of the water absorbed during soaking caused a decrease in actuator performance with no measurable actuation occurring after approximately 20 min. Upon rewetting, performance then improved, and tests were performed in approximately 1–2 min so that evaporation had little effect on the data.

The presence of water molecules in the IPMC membrane played a very important role in actuation. Actuators must remain moist for movement to occur. Water affected actuation in two ways: 1) water molecules were necessary to swell the membrane to ease the migration of ions across the membrane and 2) the movement of the water molecules helped caused the swelling/contraction within the membrane.

In a cantilevered position, actuator bending is commonly modeled as pure bending. In this manner, the deflection of the actuator can be modeled by

$$1/\rho = FL/EI \tag{5}$$

where F is the actuator tip-force output and L is the length of the neutral actuator strip.[9] E and I are the elastic modulus and moment of inertia of the actuator, respectively. Once the modulus is known for a particular metal/polymer combination, the tip force can be estimated by measuring the deflection. Equation (5) assumes that the deflection is linear.

Using this equation and the deflection measurements presented in Fig. 6, the tip force of the actuator strip was estimated and is shown in Fig. 7. E_a was assumed to be that of Nafion™. By assuming the instantaneous actuator length l was approximately equal to the length of a line drawn from the base to the actuator tip (Fig. 5), ρ was determined through geometry by

$$\rho \cong (L^2 + y^2)/2y \tag{6}$$

where L is the neutral length of the actuator.[10] A maximum tip force of approximately 0.15 mN was achieved.

The results shown in Figs. 7 and 8 both exhibit a "flat" area around zero biasing voltage. This is most likely caused by actuator

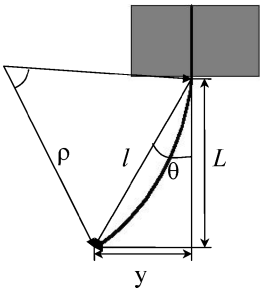

Fig. 5 Characterization parameters of the bending actuator strain.

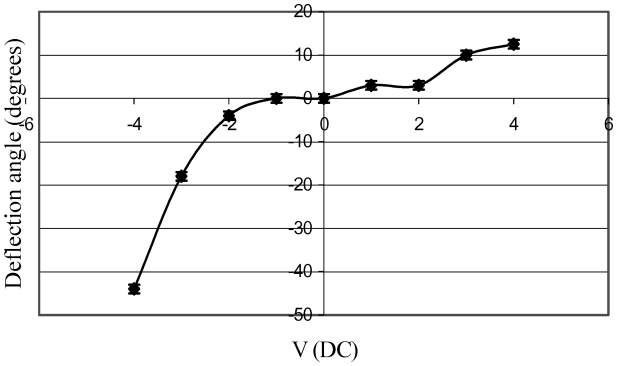

Fig. 6 Deflection angle vs biasing voltage for an IPMC actuator.

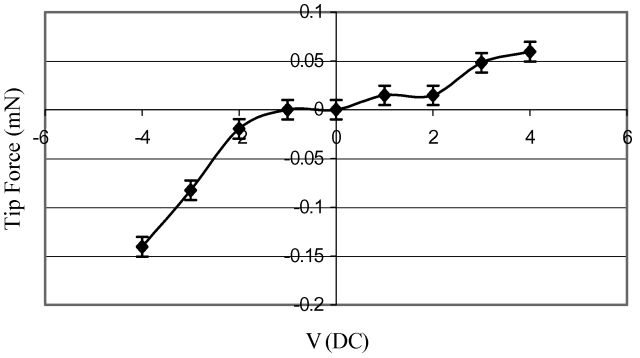

Fig. 7 Estimated tip force of the IPMC actuator for E_a = 249 MPa.

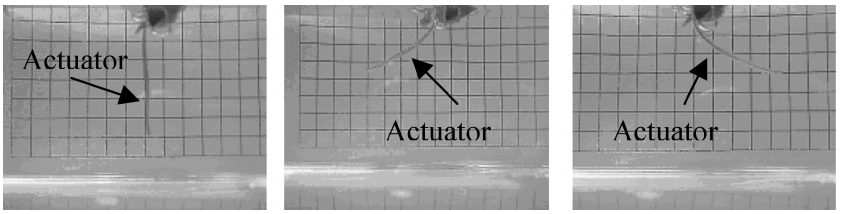

a) b) c)

Fig. 4 Bending of an IPMC actuator: a) +4 V bias, b) zero bias, and c) −4 V bias.

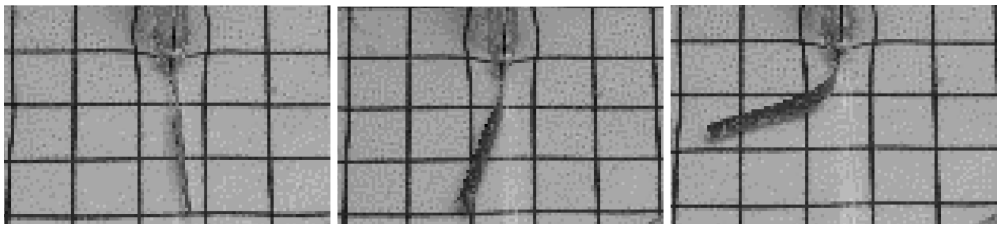

a) b) c)

Fig. 8 CP actuator in the a) oxidized position, b) initial position, and c) reduced position.

fabrication errors, as described earlier. The flat area can become an application difficulty when fine actuator control is required at low biasing voltages. To improve the actuator's performance in this voltage range, it will be necessary to fine tune the fabrication conditions and also develop a thicker actuator layer so that a larger deflection and tip force can be generated at low biasing voltages.

To determine whether the performance of the IPMC actuator satisfies the structural dynamics related constraints, the maximum axial stress and strain of the IPMC actuator were determined. The maximum axial stress of the actuator can be estimated by the tip force if the actuator "beam" is assumed to behave linearly and the centroid of the actuator $t/2$ is considered the neutral axis. For an actuator of overall thickness t,

$$\sigma \cong (FL)t/2I \tag{7}$$

where I is the total moment of inertia of actuator. The axial strain ε can be related to ρ by

$$\varepsilon \cong t/2\rho \tag{8}$$

By combining Eq. (8) with Eq. (7), the equation for axial strain becomes

$$\varepsilon \cong yt/(L^2 + y^2) \tag{9}$$

Using Eqs. (7) and (9) and the test results presented in Figs. 6 and 7, the maximum axial stress and strain of the IPMC actuator were 0.52 MPa and 0.002, respectively. Although the axial stress of the actuator compared very favorably with the stress constraint (~0.5 MPa), the axial strain was about five times smaller than the strain constraint (~0.01). This is a somewhat surprising result because IPMC is known for its strain but not for its stress output capabilities.

From Eq. (9), it is clear that the ratio of t and L largely determines the level of ε. Because of this, a thick actuator tends to result in a large axial strain, if the y deflection remains the same. The current IPMC has a thickness of 190 μm. This is about 10 times smaller than an IPMC tested by Kim and Shahinpoor,[10] who achieved an axial strain level of 0.01. From this comparison, it can be speculated that the present IPMC actuator can reach the required strain constraint of 0.01 if the actuator thickness is increased tenfold. To accomplish this will be difficult using commercially available Nafion membrane because it is only available in the range of 50–200 μm thick.

However, even wetted actuation dropped off after several weeks of testing. One possible cause for this irreversible decline in performance was the loss of functional counterions to the surrounding deionized water as a result of diffusion. To rejuvenate the actuators, several IPMC strips were soaked in a solution of 1 M $LiClO_4$ overnight. But the effort proved unsuccessful. Another possible cause was electrode delamination, but a scanning electron microscopy investigation showed no change in Au adhesion. Vacuum sputtering at high power during actuator fabrication might have degraded the Nafion, and further investigation will be necessary to determine the exact cause. The actuator characterization results presented were obtained in the first week of testing.

A critical shortcoming of the IPMC is its gradual loss of performance in a dry environment. At the Jet Propulsion Laboratory, moisture encapsulation was used in an attempt to create a dry IPMC,

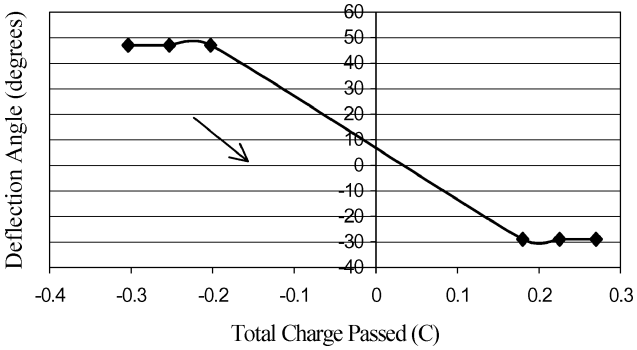

Fig. 9 Initial testing of the deflection angle of a PPy actuator with an error of ±2 deg.

but operation could only be sustained up to four months.[11] The need for moisture will most likely continue to limit the applications of IPMC in a space environment. PPy, in contrast, can use an aqueous electrolyte or a solid polymer electrolyte for operation.

CP Actuator

A 17 × 3 mm CP actuator was tested for initial, qualitative assessments. When an oxidizing current was applied, the PPy layer expanded, causing the actuator to bend in the direction of the passive polymer layer (Fig. 8a).

The expansion on oxidation was the result of the incorporation of additional dopant ions following the equation

$$PPy^0 + BF_4^- \rightarrow PPy^+BF_4^- + e^- \tag{10}$$

When a reducing current was applied, the PPy layer contracted, causing the actuator to bend in the direction of the active polymer layer (Fig. 8c). This was the result of an ion being expulsed according to the equation

$$PPy^+BF_4^- + e^- \leftrightarrow PPy^0 + BF_4^- \tag{11}$$

Because the actuator was operated in a $LiClO_4$ electrolyte, possible incorporation of ClO_4^- into the polymer matrix might also have occurred after the initial oxidation/reduction of the membrane. The deflection angle of the actuator θ was measured and is shown in Fig. 9.

Positive charge corresponds to reduction and negative charge to oxidation. A maximum angle of 29 deg was reached for 0.18 C of oxidization charge, but a much larger angle of 47 deg was reached for 0.20 C of reduction charge. This was most likely because the PPy membrane was fabricated in a mostly oxidized state. The actuator retained its oxidation state, that is, displacement, even when the electrical stimulus was removed. It did not return to the initial state until an opposite current was applied.

A simplified phenomenological model was developed by Otero and Cortès[12] to model the behavior of PPy-based actuators. The volume change of the PPy membrane depends directly on the total consumed charge q. Therefore, the applied current, or charge per unit time, governs the strain and even response time. Therefore, a

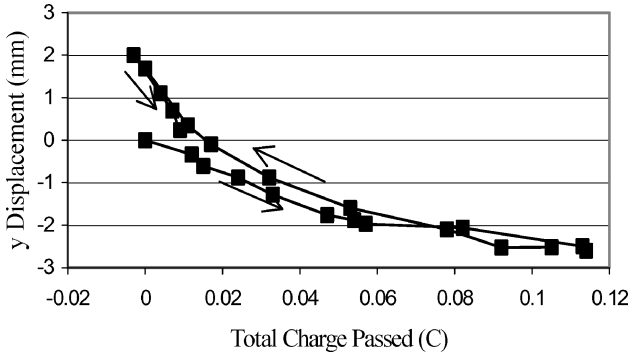

Fig. 10 Full sweep of a CP actuator with an error of ±0.02 mm.

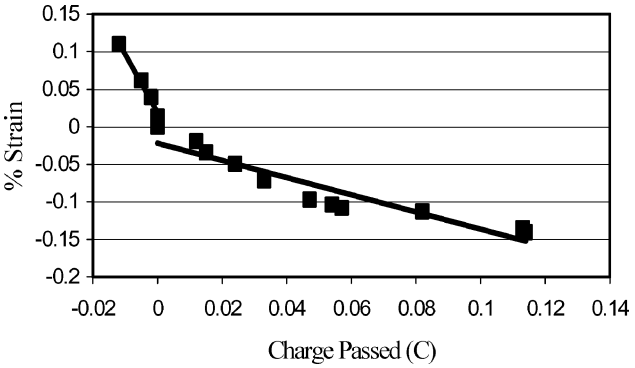

Fig. 11 Oxidation and reduction strains vs charge passed; % error in strain is 0.001.

simple equation relating the strain ε, stress output σ, and q can be written as

$$\varepsilon \cong \alpha q + \sigma / E_a \tag{12}$$

where α is a constant of units C^{-1}. For free strains, a linear relation with respect to q is expected.

Further actuator testing was conducted using a CP actuator with a length of 12.5 mm and a width of 3.5 mm. To achieve good accuracy at small deflections, the laser displacement sensor was used to measure the actuator deflection. The result of a redox cycle of the actuator is shown in Fig. 10. As can be seen, the actuator started out with no net charge and was reduced to achieve a y deflection at a rate of approximately 21 mm/C. Subsequent oxidation followed a similar path back to the neutral position, although once past the neutral position the actuator followed a path with a slope of approximately 141 mm/C. This change in slope was attributed to the increased film resistance as a result of the reduction process.[13]

To compare the experimental results with the modeling equations, axial strains achieved by the actuator were calculated using Eq. (9) and the transverse displacement results in Fig. 10. As shown in Fig. 11, the maximum linear strain obtained by this method was 0.0014 (0.14%) for 0.11 C. The axial strain calculated is about 10 times smaller than the strain constraint (~0.01).

Using the testing station, the force output capability of the actuator was also tested. Figure 12 shows the measured tip force graphed against the total charge passed. Overall, the tip force is linearly proportional to the charge passed. A maximum tip force of 2.8 mN for a charge of 0.2 C was achieved in the first run. In subsequent runs, the maximum tip force was lower.

Using Eq. (7) the present actuator was determined to have a maximum axial stress of 5.5 MPa during full oxidation. This result well exceeds the stress output constraint of 0.5 MPa. This result also compares well with the stress output of flexible piezoelectric actuators, such as PVDF (1–10 MPa)[3] but at a much lower voltage.

However, the current CP actuators can only provide small forces because of their small cross-sectional area. The development of PPy-based actuators with large cross-sectional areas is difficult. The

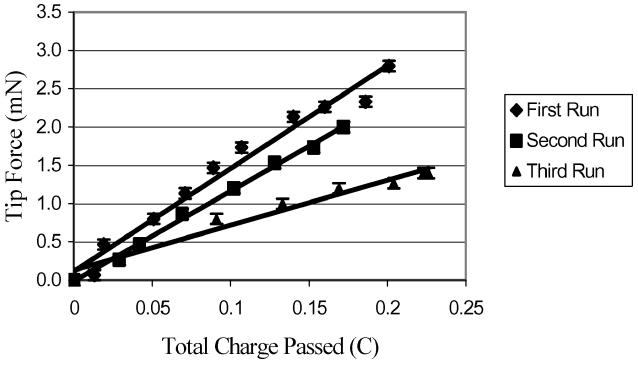

Fig. 12 Calibrated tip force for the CP actuator.

limiting factor for PPy-based actuators is the issue of scalability. The actuator length is limited by the loss of conductivity caused by reduction. Bay et al.[13] concluded that realistic effective lengths of the actuator l_{eff} were found to scale as

$$l_{\text{eff}} \propto \sqrt{t_a \eta / i_d} \tag{13}$$

where i_d is the diffusion limited current density for oxygen reduction. Realistic effective lengths for a 10-μm-thick PPy film were approximately 100 mm in the oxidized state and approximately 5 mm in the fully reduced state.[13]

According to Eq. (13), another method to increase the effective length is to increase the thickness of the membrane. Madden et al.[7] found that oxidation/reduction rates are determined by two factors: RC charging and ion diffusion. During dc cycling, PPy behaves electrically as a capacitor, charging and discharging during electrochemical cycling. The resistance of the electrolyte dominates the overall resistance of the electrochemical circuit, so that a RC time constant can be expressed as

$$\tau_{\text{RC}} = R_e \cdot C_V \tag{14}$$

At intermediate to high frequencies, switching times are limited by the diffusion of dopant ions. The diffusion time constant can be expressed as

$$\tau_D = t_a^2 / 4D \tag{15}$$

Therefore, very thick membranes are self-limiting, and special configurations would be necessary to produce large forces.

Conclusions

With the maximum stress and strain of the electroactive-polymer (EAP) actuators determined, their effectiveness in controlling space inflatable structures was evaluated by comparing the numbers with the stress and strain output requirements. In terms of stress, it is clear that both the ionic-polymer-metal-composite (IPMC) and conductive-polymer (CP) actuators meet the requirement of 0.5 MPa. However, in terms of strain, neither the IPMC nor the CP actuators can output a high enough level to meet the required level of 0.008. Whereas the IPMC actuator's strain is five times smaller than the requirement, the CP actuator's is almost 10 times smaller. This is a somewhat surprising result because EAP actuators are known for their strain and not for their stress capability. Nonetheless, based on this study it can concluded that a composite actuator design (consisting of multiple EAP layers or strips perhaps) with a much higher strain capability than the current simple designs will be necessary in order to successfully apply EAP actuator technology to space inflatable structures.

Acknowledgment

This project is sponsored by NASA Jet Propulsion Laboratory through Contract 1221424.

References

[1]Amimoto, S. T., Mason, A. J., and Wise, K., "MEMS-Based Sensing Systems: Architecture, Design, and Implementation," *Microengineering Aerospace Systems*, edited by H. Helvajian, Aerospace Press, El Segundo, CA, 1999, pp. 389–448.

[2]Jenkins, C. H. M., and Vinogradov, A. M., "Active Polymers for Space Applications," *IEEE Aerospace Conference Proceedings*, Vol. 7, Inst. of Electrical and Electronics Engineers, Piscataway, NJ, 2000, pp. 415–420.

[3]Wax, S. G., and Sands, R. R., "Electroactive Polymer Actuators and Devices," *Proceedings of SPIE Smart Structures and Materials—Electroactive Polymer Actuators and Devices (EAPAD)*, Vol. 3669, edited by Y. Bar-Cohen, Society of Photo-Optical Instrumentation Engineers, Bellingham, WA, 1999, pp. 2–10.

[4]Slade, K. N., and Tinker, M. L., "Analytical and Experimental Investigation of the Dynamics of Polyimide Inflatable Cylinders," *Proceedings of the 40th Structures, Structural Dynamics, and Materials Conference*, Vol. 4, AIAA, Reston, VA, 1999, pp. 2495–2506.

[5]Chaudhry, Z., and Rogers, C. A., "The Pin-Force Model Revisited," *Journal of Intelligent Material Systems and Structures*, Vol. 5, No. 3, 1994, pp. 347–354.

[6]Freeland, R. E., Bilyeu, G. D., and Mikulas, M. M., "Inflatable Deployable Space Structures Technology Summary," International Astronautical Federation, Paper 1501, Sept. 1998.

[7]Madden, J. D. W., Madden, P. G. A., and Hunter, I. W., "Polypyrrole Actuators: Modeling and Performance," *Proceedings of SPIE Smart Structures and Materials—Electroactive Polymer Actuators and Devices (EAPAD)*, Vol. 4329, edited by Y. Bar-Cohen, Society of Photo-Optical Instrumentation Engineers, Bellingham, WA, 2001, pp. 72–83.

[8]de Gennes, P. G., Okumura, K., Shahinpoor, M., and Kim, K. J., "Mechanoelectric Effects in Ionic Gels," *Europhysics Letters*, Vol. 50, No. 4, 2000, pp. 513–518.

[9]Bar-Cohen, Y., and Leary, S., "Electro Active Polymers (EAP) Characterization Methods," *Proceedings of SPIE Smart Structures and Materials—Electroactive Polymer Actuators and Devices (EAPAD)*, Vol. 3987, edited by Y. Bar-Cohen, Society of Photo-Optical Instrumentation Engineers, Bellingham, WA, 2000, pp. 12–16.

[10]Kim, K. J., and Shahinpoor, M., "Development of Three-Dimensional Polymeric Artificial Muscles," *Proceedings of SPIE Smart Structures and Materials—Electroactive Polymer Actuators and Devices (EAPAD)*, Vol. 4329, edited by Y. Bar-Cohen, Society of Photo-Optical Instrumentation Engineers, Bellingham, WA, 2001, pp. 223–237.

[11]Bar-Cohen, Y., Leary, S., Oguro, K., Tadokoro, S., Harrison, J., Smith, J., and Su, J., "Challenges to the Transition of IPMC Artificial Muscle Actuators to Practical Application," *Materials Research Society Symposium Proceeding*, Vol. 600, 1999, p. 567.

[12]Otero, T. F., and Cortés, M. T., "Characterization of Triple Layers," *Proceedings of SPIE Smart Structures and Materials—Industrial and Commercial Applications of Smart Structures Technologies*, Vol. 4332, edited by A.-M. McGowan, Society of Photo-Optical Instrumentation Engineers, Bellingham, WA, 2001, pp. 93–100.

[13]Bay, L., West, K., Vlachopoulos, N., and Skaarup, S., "Potential Profile in a Conducting Polymer Strip," *Proceedings of SPIE Smart Structures and Materials—Electroactive Polymer Actuators and Devices (EAPAD)*, Vol. 4329, edited by Y. Bar-Cohen, Society of Photo-Optical Instrumentation Engineers, Bellingham, WA, 2001, pp. 54–58.

M. Lake
Associate Editor